Helical Gold Nanotube Synthesized at 150 K

Yoshifumi Oshima* and Akiko Onga
Department of Materials Science & Engineering, Tokyo Institute of Technology, 4259 Nagatsuta, Midori-ku, Yokohama 226-8502 Japan

Kunio Takayanagi
Department of Physics, Tokyo Institute of Technology, Oh-okayama, Meguro-ku, Tokyo 152-8551 Japan
(Received 16 April 2003; published 13 November 2003)

Gold nanowires were synthesized at 150 K by electron beam thinning of a gold thin foil in an UHV electron microscope. The gold nanowires were found to have a helical multishell structure (HMS). One particular nanowire, which was thinner than the 7-1 HMS nanowire, was found to have a tubular structure. The gold single wall nanotube is composed of five atomic rows that coil about the tube axis. The diameter was 0.4 nm and the pitch was 11 nm. The stability of the (5, 3) nanotube was discussed in terms of the shear deformation of the triangular network of gold atoms.

DOI: 10.1103/PhysRevLett.91.205503 PACS numbers: 61.46.+w, 68.37.Lp, 68.65.La

Nanowires and nanotubes have raised much interest by virtue of their unique physical and chemical properties owing to their helical structures. Single wall carbon nanotubes (SWNTs) [1] have metallic or semiconductive properties depending on the chirality due to quantization of electron waves along the circumference of the tube [2,3]. SWNTs and multiwall nanotubes (MWNT) have a wide range of applications, such as p-n junctions [4], rectification [5], and field-effect transistor (FET) devices [6,7]. Tubular structures of boron nitride (BN) [8–10] also have unique electronic and mechanical properties [8]; they are semiconductive with a gap of roughly 5.5 eV independent of the tube diameter and chirality [11]. Tubular structures of layered compounds such as molybdenum disulfide (MoS_2) and tungsten disulfide (WS_2) have also been synthesized [12]; these can be metallic or semiconductive [13].

Metal nanowires show conductance quantization in units of $2e^2/h$ [14–18]. A single strand of gold atoms was confirmed to have a unit conductance [18,19]. Long gold nanowires thinner than 2 nm have recently been synthesized in an UHV electron microscope [20]. These gold nanowires have a helical multishell (HMS) structure. The n-n' HMS nanowire is composed of two coaxial tubes, whose outer and inner tube have n and n' atomic rows of gold atoms, respectively. The atomic rows coil about the tube axis. Their atomic geometry resembles that of the multiwall carbon nanotube (CNT), when the honeycomb network of carbon atoms in the CNT is replaced by a triangular network of gold atoms (Fig. 1) [20–22]. The triangular network is deformed by the shear strain ϵ. The shear deformation changes the helical pitch (L) and diameter (D) of the HMS nanowire.

Theoretical studies predict a multiwall tubular structure for metal nanowires: Molecular dynamic simulation revealed a tubular geometry for gold [23] and helical weird geometry for lead [24]. More recently, force calculations for the gold 7-1 HMS structure, or the (7, 4) tube plus one atomic row at the center of the tube [21], confirmed the n-n'-n'' HMS nanowire ($n \geq 7$) structure. Although significant progress has been made on geometry and quantized conductance of gold nanowires [25], the existence of gold SWNT has not been theoretically shown yet [21,26]. In experiments, platinum (6, 3) SWNT was

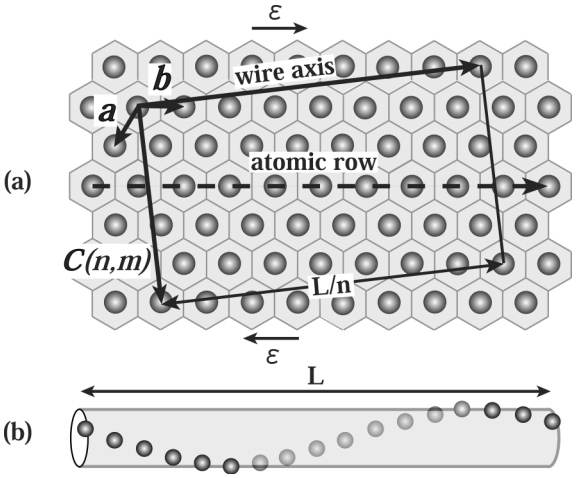

FIG. 1. (a) A sheet of the triangular network of gold atoms that forms coaxial tubes of the HMS nanowire. Large circles show gold atoms. **a** and **b** indicate the basic vector of the triangular network. The gold atomic row has a nearest neighbor atom distance of 0.29 nm. The triangular network is deformed by shear strain ϵ in the **b** direction. $\mathbf{C}(n, m)$ is the chiral vector, defined as $\mathbf{C}(n, m) = n\mathbf{a} + (m + n\epsilon/2)\mathbf{b}$. $\mathbf{C}(n, m)$ in the figure is $\mathbf{C}(5, 3)$ for the gold (5, 3) nanotube. The diameter of the tube, D, is given by $D = |\mathbf{C}(n, m)|/\pi$. (b) The helical pitch, L, of the nanotube is given by $L = |\mathbf{C}(n, m)|/\tan\theta$, where θ is the angle between the atomic row (parallel to the **b** direction) and the tube axis. The atomic row rotates by 2π radians when it translates in the tube axis by the helical pitch, L.

found to form at 700 K [27], while no gold SWNT formation was observed.

In the present study, we report experimental evidence for gold SWNT, synthesized at 150 K in an UHV electron microscope. The thinnest gold nanowire, 0.4 nm in diameter, was found to be the (5, 3) nanotube, composed of five atomic rows that coil with a helical pitch of 11 nm.

To synthesize gold nanowires in an UHV electron microscope (JEM 2000FXV) [28], a homemade specimen holder was used to cool the nanowires to as low as 120 K [29]. A 2-nm-thick gold film was prepared by vacuum deposition on a thick silver (001) film predeposited on a NaCl substrate [30]. After dissolving the silver film and the NaCl substrate, we mounted the gold film on a homemade carbon microgrid. The gold film was then irradiated by an intense electron beam (beam density: 100 A/cm^2; beam energy: 200 keV) in order to clean and thin the film under a vacuum of 10^{-7} Pa in the UHV electron microscope. After several hours of irradiation, a large number of holes were created in the film, the bridge between adjacent holes becoming increasingly narrow. The specimen was then cooled to 150 K, and the beam intensity was reduced to ~50 A/cm^2. When the bridge turned into a nanowire with a diameter of around 2 nm, the beam intensity was reduced further (30 A/cm^2) to slow down the thinning speed. The structure of the gold nanowires were videotaped at atomic resolution at 33-ms intervals. As the temperature dropped below room temperature, the gold nanowires became harder to break. On the other hand, they were shortened due to suppression of the diffusion. Thus, we performed the experiment at 150 K.

The gold nanowires formed at 150 K were confirmed to have a helical multishell (HMS) structure that has been reported at room temperature [20]. The apparent width of the nanowires changed in steps in a manner similar to that reported in Fig. 2 of Ref. [20]. The transmission electron microscope (TEM) images were reproduced well by the image simulation [31]. Figures 2(a) and 2(b) show TEM images of gold nanowires with an apparent width of 0.56 and 0.8 nm, respectively. Image simulation revealed that the four spotty dark lines in Fig. 2(a) could be reproduced well by the 11-4 HMS structure model that consists of the (11, 6) outertube and (4, 2) innertube. The three spotty lines in Fig. 2(b) were reproduced by the 7-1 HMS structure that consists of the (7, 4) tube and a single atomic row at the center of the (7, 4) tube. The spotty dark lines in the 11-4 HMS and 7-1 HMS nanowires were not straight, but rather wavy. The wavy modulation of the line image is due to the helical structure of the atomic rows that coil around the tube axis [Fig. 1(b)]. The period of modulation corresponds to L/n for the n-n' HMS nanowire. Based on several TEM images, the helical pitch of the 11-4 HMS and 7-1 HMS were determined to be in the range of 65–75 nm and 26–28 nm, respectively. The shear strain (ϵ) in the gold (111) atomic sheet is determined to be between -0.018 and -0.028 for the (11, 6) tube of the 11-4 HMS, and between -0.026 and -0.036 for the (7, 4) tube of the 7-1 HMS. The observed shear strains at 150 K are rather negative, consistent with the values reported at 300 K: The pitch of the 11-4 HMS formed at 300 K was 84 nm ($\epsilon = -0.034$) and that of the 7-1 HMS was 28 nm ($\epsilon = -0.036$) [20].

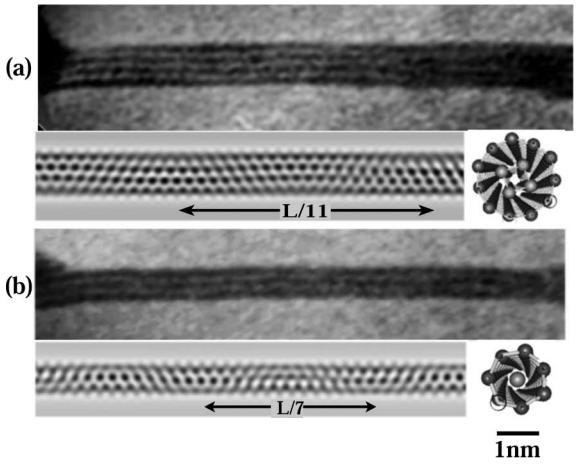

FIG. 2. TEM images of (a) 11-4 helical multishell (HMS) gold nanowire and (b) 7-1 HMS nanowire synthesized at 150 K. Images are reproduced from a video recording of the thinning process. The number of spotty dark lines is four in (a), and three in (b). The simulated image and the model (viewed from the HMS axis) are shown for each TEM image. The image simulation was performed by multislice calculation [31] for 200 kV (accelerating voltage), $C_s = 0.7$ mm (spherical aberration), $C_c = 1.2$ mm (chromatic aberration), $\Delta E = 10^{-6}$ (voltage and lens stability), $\Delta f = -55$ nm (under focus of the objective lens), and a beam divergence of 3.4 mrad. The convergent beam illumination (CBI) condition was used for the simulation program [32]. L/n indicates the period of the wavy modulation; $L/11 = 5.9$ nm for (a) and $L/7 = 4$ nm for (b).

Further thinning changed the gold nanowires in the manner shown in Fig. 3. Figure 3(a) is the TEM image of two spotty dark lines, and Fig. 3(b) is that of a single spotty dark line: they lasted for ten and a few seconds, respectively. We measured the spacing of the two dark lines in Fig. 3(a) and those of several other TEM images reproduced from the videotape. The spacing modulated along the nanowire; we obtained an average value of ~0.25 nm. In order to determine the structure of the gold nanowires showing the two spotty dark lines, we performed an image simulation for the (n, m) tubes under shear deformation. For each n ($n = 6, 5, 4, 3$), we chose m such that $n > m \geq n/2$. The shear strain of the triangular network in the b direction (see also Fig. 3 of Ref. [20]) was chosen in the range $-0.05 < \epsilon < +0.1$. The nearest neighbor distance of the triangular network of gold atoms was chosen to be 0.29 nm after the experiment. The defocus values were chosen to be -50, -55, and -60 nm. After elaborate simulations, we confirmed that the spacing of the spotty dark lines was largely independent of the

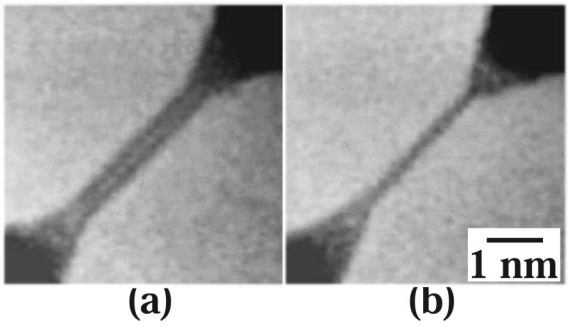

FIG. 3. A series of TEM images of the thinning process of a gold nanowire at 150 K. (a) A newly observed gold nanowire showing two spotty dark lines, ~0.25 nm apart. (b) A single strand of 11 gold atoms. This will be described in detail elsewhere.

values of the defocus and shear strain. The spacing was rather modulated along the tube because of the helical structure: The spacing modulation for the (6, 3) nanotube was 0.43 ~ 0.48 nm, while that for the (5, 3) nanotube was 0.24 ~ 0.29 nm. A comparison of the spacing for all the (n, m) tube models revealed the (5, 3) nanotube to be the best candidate.

The model for the (5, 3) gold nanotube is shown in Fig. 4(a). The diameter of the tube is 0.40 nm and the helical pitch is 11 nm (for $\epsilon = 0.005$). Figures 4(b) and 4(c) are side views of the model and the simulated image, respectively. Figure 4(d) is the observed high-resolution image of the gold nanotube. The simulated image reproduces characteristic patterns of the observed image: The hexagonal patterns [five dark dots at A and B in (b) and (c)] appear locally, and they rotate periodically along the tube. By comparison of (b) with (c), we find that the dark dots appear at the positions where two gold atoms are superposed in the direction of the incident electron beam. The superposition results from the tubular geometry, and the hexagonal pattern rotates periodically due to the helical structure of the gold atomic rows [Fig. 1(b)]. Based on the fact that the rotation occurs at every distance of $L/10$, the observed helical pitch was determined to be 11 nm. For several TEM images, the helical pitches gave positive shear deformation in the range of $0 < \epsilon < 0.01$.

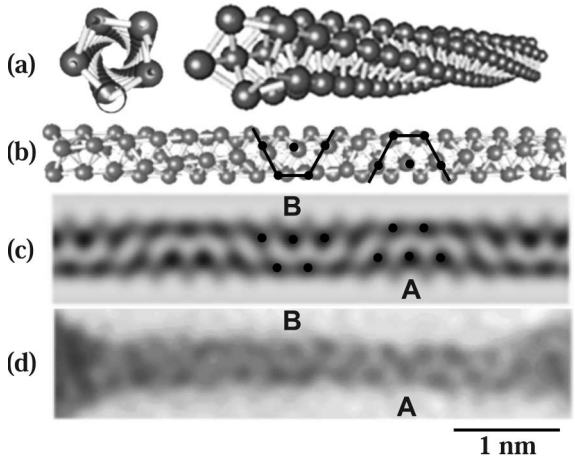

FIG. 4. (a) Structure model for the gold (5, 3) nanotube; (b) side view of the tube with a diameter of $D = 0.40$ nm and a helical pitch of $L = 11$ nm (for $\epsilon = 0.005$); (c) simulated image; and (d) observed TEM image. In the TEM image, spatial frequencies above 0.16 nm have been filtered out. The local hexagonal patterns (marked by A and B) are shown by dots and lines in (b) and (c). The distance between pattern A and B is about 1.1 nm.

Tosatti *et al.* were the first to report on weird wires that have a noncrystalline structure. They showed that weird wires appear for Pb and Al below a critical diameter to reduce the edge energy of the crystalline wire [24]. Indeed, gold nanowires exhibit a hexagonal prism geometry above 2 nm [33]. Recent theoretical work [21] proved that the 7-1 HMS nanowire is the energetically stable structure for gold and platinum. However, no predictions on n-0 HMS nanowires, that is (n, m) nanotubes, have been made.

Sen *et al.* theoretically discussed the stability of pentagonal nanowires [26]. Their pentagonal R geometry corresponds to the present (5, 5) tube, and the pentagonal S geometry corresponds to a (5, 5) tube with an atomic strand at its hollow center. According to their calculation for gold, the R geometry is more stable than the S geometry, and a deformed R geometry also has better stability than the S geometry. Those pentagonal nanowires appear for Pb (B4 structure in Ref. [24]) and Al (A6 structure in Ref. [24]). The gold nanotubes in the present experiment do not have a (5, 5) tube, but a (5, 3) tube. The (5, 3) nanotube has not been studied theoretically.

We assume that the gold (5, 3) nanotube is formed by the excess elastic energy rolling up the (111) atomic sheet in order to show that the tube has a local energy minimum for a positive, rather than negative, shear deformation. A single gold (111) atomic sheet seems to be stable based on the following experimental facts: The gold (100) film transforms into a (111) film below the critical film thickness (ca. 8 atomic layers), and the (111) film is thinned further layer by layer [34]. The gold (001) surface reconstructs to a hexagonal lattice [35]. Thus, we regard the sheet as an elastic continuum of thickness, d. Because of the shear deformation ϵ, the elastic energy increases by $(G/6)\epsilon^2$ per unit volume of the sheet, where G is the shear rigidity. To form a tube of diameter D, the elastic energy increases by $(E/3)(d/D)^2$ per unit volume, where E is the Young's modulus [36]. No volume dilatation is induced during the course of the deformations. Based on the cohesive energy, E_c, of the gold atom (=3.78 eV in Table III of Ref. [37]), the energy, $E(\epsilon)$, of the (5, 3) gold tube per atom is described by the following equation:

$$E(\epsilon) = -E_c + \Omega\{(E/6)(d/D)^2 + (G/6)\epsilon^2\}, \quad (1)$$

where $\Omega = (\sqrt{3}/2)d^3$ is the atomic volume occupied by a gold atom. Taking $E = 8.0 \times 10^{10}$ and $G = 2.8 \times 10^{10}\ \mathrm{N/m^2}$ for the bulk gold crystal [38], $E(\epsilon) = -3.78 + 0.91(1 - 0.13\epsilon) + 0.61\epsilon^2$, which gives a local minimum at $\epsilon = 0.097$. Although this ϵ value is unrealistic, the (5, 3) tube was shown to have a local minimum at a positive value. Also, we estimated the cohesive energy of the (5, 3) tube using the glue model [37]. The (5, 3) tube with $\epsilon = 0$ was found to have a cohesive energy of 1.78 eV. The contribution of the second nearest neighbor bonds (bond length $\sim$0.38 nm), due to rolling of the sheet, is 0.02 eV. As ϵ increased to 0.05, the energy of the (5, 3) tube changed by less than 0.01 eV. Thus, we did not further pursue the determination of the ϵ value that yields a local minimum in the energy of the (5, 3) tube.

The observed values of ϵ for the n-n'-n'' HMS nanowires (present result and Table I in Ref. [20]) with negative values were driven by taking the misfit energy between the outer and inner tubes. According to the misfit energy of epitaxial films [39], the gold atomic sheets for the outer and inner tubes form a twisted interface, which is caused by the difference in the angle of atomic rows, $\theta - \theta'$, (Fig. 1) of the outer and inner tube [40]. In order to lower the misfit energy, the outer (n, m) tube (where n is an odd number) has to have a negative strain to reduce the angle difference with the inner (n', m') tube (where n' is an even number). Thus, HMS nanowires have negative strains in their outer nanotubes.

Although dedicated atomic theories are needed, the shear strain, ϵ, of the (111) gold atomic sheet was shown to play an important role in giving a local minimum in the energy of the gold (5, 3) nanotube.

In conclusion, we synthesized a gold nanotube at 150 K. The gold (5, 3) nanotube had five helical atomic rows that coiled around the tube axis with a 11-nm pitch.

This work was supported by the Ministry of Education, Culture, Sports, Science and Technology of Japan (Quantum Contact: No. 12002005).

*Electronic address: ohshima@materia.titech.ac.jp

[1] S. Ijima, Nature (London) **354**, 56 (1991).
[2] R. Saito *et al.*, Appl. Phys. Lett. **60**, 2204 (1992).
[3] N. Hamada, S. I. Sawada, and A. Oshiyama, Phys. Rev. Lett. **68**, 1579 (1992).
[4] F. Léonard and J. Tersoff, Phys. Rev. Lett. **83**, 5174 (1999).
[5] P. G. Collins, M. S. Arnold, and Ph. Avouris, Science **292**, 706 (2001).
[6] S. J. Tans, A. R. M. Verschueren, and C. Dekker, Nature (London) **393**, 49 (1998).
[7] R. Martel *et al.*, Appl. Phys. Lett. **73**, 2447 (1998).
[8] A. Rubio, J. L. Corkill, and M. L. Cohen, Phys. Rev. B **49**, 5081 (1994).
[9] E. Bengu and L. D. Marks, Phys. Rev. Lett. **86**, 2385 (2001).
[10] D. Golberg *et al.*, Chem. Phys. Lett. **308**, 337 (1999).
[11] X. Blase *et al.*, Europhys. Lett. **28**, 335 (1994).
[12] R. Tenne, M. Homyonfer, and Y. Feldman, Chem. Mater. **10**, 3225 (1998).
[13] G. Seifert *et al.*, Phys. Rev. Lett. **85**, 146 (2000).
[14] J. I. Pascual *et al.*, Phys. Rev. Lett. **71**, 1852 (1993).
[15] N. Agraït, J. G. Rodrigo, and S. Vieira, Phys. Rev. B **47**, 12 345 (1993).
[16] L. Olesen *et al.*, Phys. Rev. Lett. **72**, 2251 (1994).
[17] C. J. Muller, J. M. van Ruitenbeek, and L. J. de Jongh, Phys. Rev. Lett. **69**, 140 (1992).
[18] A. I. Yanson *et al.*, Nature (London) **395**, 783 (1998).
[19] H. Ohnishi, Y. Kondo, and K. Takayanagi, Nature (London) **395**, 780 (1998).
[20] Y. Kondo and K. Takayanagi, Science **289**, 606 (2000).
[21] E. Tosatti *et al.*, Science **291**, 288 (2001).
[22] Y. Oshima, Y. Kondo, and K. Takayanagi, J. Electron Microsc. **52**, 49 (2003).
[23] G. Bilalbegović, Phys. Rev. B **58**, 15 412 (1998).
[24] O. Gülseren, F. Ercolessi, and E. Tosatti, Phys. Rev. Lett. **80**, 3775 (1998).
[25] E. Tosatti and S. Prestipino, Science **289**, 561 (2000).
[26] P. Sen *et al.*, Phys. Rev. B **65**, 235433 (2002).
[27] Y.Oshima *et al.*, Phys. Rev. B **65**, 121401(R) (2002).
[28] K. Takayanagi *et al.*, Jpn. J. Appl. Phys. **26**, L957 (1987).
[29] Y. Oshima *et al.*, Surf. Sci. **476**, 107 (2001).
[30] D. W. Pashley, Adv. Phys. **5**, 173 (1956).
[31] J. M. Cowley and A. F. Moodie, Acta Crystallogr. **10**, 609 (1957).
[32] M. Mitome and K. Takayanagi, Ultramicroscopy **33**, 255 (1990).
[33] Y. Kondo and K. Takayanagi, Phys. Rev. Lett. **79**, 3455 (1997).
[34] Y. Kondo, Q. Ru, and K. Takayanagi, Phys. Rev. Lett. **82**, 751 (1999).
[35] F. Ercolessi, M. Parrinello, and E. Tosatti, Phys. Rev. Lett. **57**, 719 (1986).
[36] K. Kanamitsu and S. Saito, J. Phys. Soc. Jpn. **71**, 483 (2002).
[37] F. Ercolessi, M. Parrinello, and E. Tosatti, Philos. Mag. A **58**, 213 (1988).
[38] *American Institute of Physic Handbook*, edited by D. E. Gray (McGraw-Hill, New York, 1972), 3rd ed., pp. 2–60.
[39] J. H. van der Merwe, Proc. Phys. Soc. London Sect. A **63**, 616 (1950).
[40] K. Takayanagi and Y. Kondo (unpublished).